

Department of Electrical
and
Computer Systems Engineering

Technical Report
MECSE-13-2004

Implementation and characterization of mode-locked fiber
lasers

Lam Quoc Huy Le Nguyen Binh

MONASH
UNIVERSITY

Implementation and characterization of mode-locked fiber lasers

Lam Quoc Huy & Le Nguyen Binh
Department of Electrical and Computer Systems Engineering
Monash university, Clayton, Victoria 3168, Australia

Abstract

This paper presents the implementation of several mode-locked fiber lasers employing active harmonic mode locking, rational harmonic mode locking, and regenerative mode locking techniques. The effects of the cavity settings on the characteristic of the lasers have been studied. It is found that pulse train with short pulse width can be obtained by modulating the lightwave with high modulation frequency, deep modulation depth and incorporating a wide bandwidth filter into the ring cavity. High pump power and long fiber length ring cavity also help to shorten the pulse via the soliton effect. Rational harmonic mode-locking techniques can be applied to increase the pulse repetition rate via the multiplication effect when detuning the modulation frequency. However, the output pulse train of the RHMLFL experiences amplitude fluctuation from pulse to pulse unless amplitude equalization is applied in the ring cavity. Furthermore we have also observed a new phenomenon in which ultra high peak pulse train is generated when the modulation frequency is detuned by about 10 kHz. The underlying physical mechanism has still not been explained but we believe that the super-mode competition and the relaxation time of the optical amplification in the ring may be the reasons for this phenomenon.

Detailed numerical studies of several mode-locked fibre lasers have also been reported and posted on the same website. The experimental results reported hereunder consistently agree with numerical simulated pulse sequences.

1 Introduction

Mode locking is a technique used to produce a periodic train of multi-modes laser pulses with high peak value and short pulse width by forcing the phases of the modes to maintain their relative values. The first mode locking laser was demonstrated by Gürs and Müller [1] in a Ruby laser and the mechanism of mode locking was first clearly explained by DiDomenico and Yariv [2]. The method Gürs and Müller used in their laser is referred to as active mode locking, in which an internal modulator is incorporated into the laser cavity. The modulator is driven by an external periodic wave to force the phases of the multi modes to be coherent and thus form a periodic pulse train in the laser. Another method, the passive mode locking, was then introduced in 1967 by Mocker and Collin [2] in which a saturable absorber was used to suppress low intensity pulses but enhance the high intensity lasing ones. The result is that the total energy reflecting back and forth in the lasing cavity cluster into a train of very narrow-width pulses.

The potential to produce very short pulses of mode locked laser attracted many research laboratories. Many techniques have been developed to shorten the pulse width of the mode locked laser. Sub-picosecond pulses were generated by Shank and Ippen using passive mode locked continuous (CW) dye laser in 1974 [3]. In 1981, Fork et al produced a technique called colliding pulse mode-locking [4] to compress the pulse to shorter than 0.1 ps. Femto-second pulses were attained in 1984 by Fujimoto et al [5]. Then six-femto-second pulses were generated by Fork et al. in 1987 using third order nonlinear phase compensation [6]. And a record of shortest pulse of about 5 fs was achieved by Morgner et al. in 1999 using dispersion managed soliton laser [7].

Recently, active harmonic mode-locked fiber laser has attracted great interest due to its ability to produce stable optical pulse train with very short pulse width and at high repetition rate [8-12]. Although many papers have been reported to demonstrate techniques to improve the performance of the lasers, there is no paper about the performance of the lasers under difference settings of the laser cavity. This paper therefore presents the implementation and characterization of the active harmonic mode-locked fiber laser for studying the affects of the cavity setting on the performance of the output pulses.

In active harmonic mode-locked fiber lasers, the optical modulator is the critical photonic component for locking the harmonics of the resonant spectrum into a particular longitudinal mode. Therefore, it is very important to characterize the optical modulator. Section 2 thus presents the biasing and optical transmission transfer characteristics of a Mach-Zehnder interferometric modulator.

Similarly an EDF optical amplifier is also constructed and characterized as described in Section 3. The dependence of the gain on the signal wavelength, signal input power and pump power will be explored.

Section 4 presents the implementation of the harmonic mode-locked laser. The effects of modulation frequency, modulation depth, pump power for EDFA and fiber ring length are studied. Rational harmonic mode-locking for multiplication of repetition rate is also demonstrated in Section 4 followed by the regenerative harmonic mode-locked laser. We also report an observation of “giant” pulse trains (a peak power of 500 mW) generated from a harmonic mode locked laser when the modulation frequency is detuned by about 10 kHz.

2 Measurement of MZI modulator transmission function

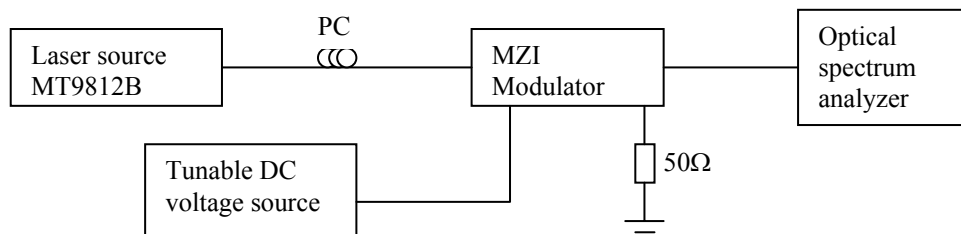


Figure 1 - MZI modulator measurement setup

Figure 1 shows the experimental setup for measuring the MZI modulator transmission function (optical transfer characteristics which is defined in Eq 4). The optical source, extracted from a tunable laser MT9812B, is fed to the input of the MZI modulator through a polarization controller. The fiber polarization controller (PC) is used to rotate the input polarization of the lightwaves coupled to the diffused channel waveguide of the interferometric intensity modulator of MZI modulator. The MZI modulator is the Sumitomo Cement Company SCC MZ2-78-20-453, whose bandwidth is around 20 GHz.

The output of the MZI modulator is connected to an Anritsu AQ6317B optical spectrum analyzer for measuring the output power. The 50Ω termination is used for matching the RF traveling waves and has no effect in this measurement.

The MZI modulator transmission characteristic is measured at 1550nm which is the central wavelength of the C-band. The output power of the laser source is set at 10 dBm. Table 1 shows the output powers of the MZI modulator at different values of the bias voltage V_{bias} . Using the tabulated results, we can determine the following parameters of the modulator:

$$V_{\pi} = V_{biasMax} - V_{biasMin} = 0.4 - (-3.8) = 4.2 V \quad (1)$$

$$Extinction\ ratio = P_{outMax} - P_{outMin} = 2 - (-23.9) = 25.9dB \quad (2)$$

$$Insertion\ loss\ (IL) = P_{in} - P_{outMax} - L_{pc} = 10 - 2 - 3 = 5dB \quad (3)$$

where $V_{biasMax}$ is the bias voltage applied to obtain maximum output power; likewise the $V_{biasMin}$ is for minimum output power, L_{pc} : Polarization controller insertion loss

The above parameters are compared with those specified by the manufacturer. The followings are the parameters supplied from the manufacturer: $V_{\pi} = 4.8V$, extinction ratio $ER = 28dB$, insertion loss $IL = 3.7dB$. Hence there is a small degradation of the modulator in the extinction ratio and the modulator insertion loss. A small change of the value of V_{π} is noted. This could be due to the aging effect of the optical diffused waveguides. The DC drift of the applied DC voltage is also recorded. The maximum transmission is occurred at 0.4V rather than at 0 V.

The normalized optical transmittance (transmission function) of the modulator is defined as:

$$T = \frac{I_0}{AI_I} = \frac{P_{out}}{P_{out\ max}} \quad (4)$$

where I_0 and I_I are the output and input intensity respectively. A is a constant accounted for the insertion loss of the modulator.

Vbias(V)	-4.5	-4.2	-4	-3.8	-3.5	-3.3	-3	-2.8	-2.5	-2.25
P_{out}(dBm)	-6.7	-10	-15.7	-23.9	-18.2	-12.8	-8	-6.5	-4.2	-2.9
P_{out}(mW)	0.21	0.1	0.03	0	0.02	0.05	0.16	0.22	0.38	0.51
T	0.13	0.06	0.02	0	0.01	0.03	0.1	0.14	0.24	0.32

(a)

Vbias(V)	-2	-1.5	-1	-0.5	0	0.4	1	1.5	2	2.5
P_{out}(dBm)	-2	-0.3	1	1.6	1.9	2	1.9	1.6	1.4	1
P_{out}(mW)	0.63	0.93	1.26	1.45	1.55	1.58	1.55	1.45	1.38	1.26
T	0.4	0.59	0.79	0.91	0.98	1	0.98	0.91	0.87	0.79

(b)

Table 1- MZI modulator transmission function measurement result

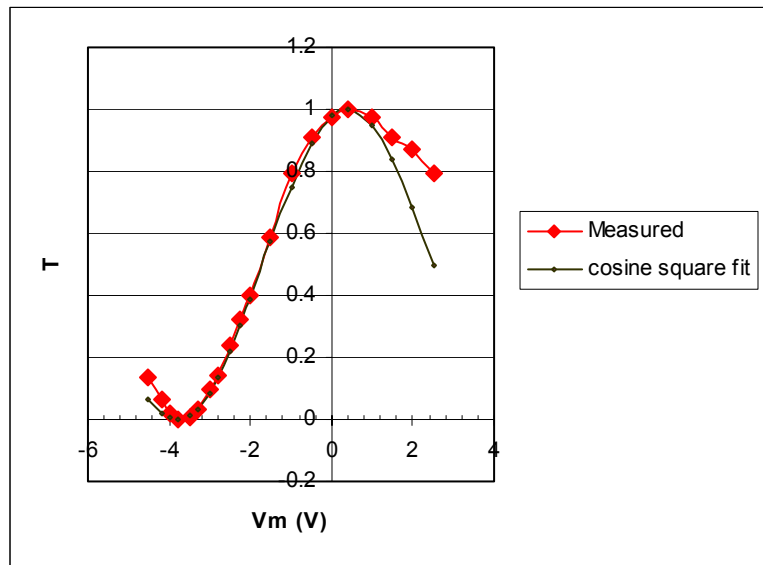


Figure 2 - MZI Modulator normalized optical output intensity as a function of the DC voltage applied to the waveguide electrodes

The measured and the theoretical \cos^2 fit transmission function of the MZI modulator are shown in Figure 2. Hence the modulator transmission function can be approximated by a \cos^2 profile:

$$T = \cos^2\left(\frac{\pi(V_m - V_{sh})}{2V_\pi}\right) = \cos^2\left(\frac{\pi(V_m - 0.4)}{8.4}\right) \quad (5)$$

3 EDFA measurement

An Erbium-doped Fiber Amplifier (EDFA) has been constructed and tested. The EDFA consists of a 16 m long erbium-doped fiber, two WDM 980/1550 couplers, two isolators, and two 980 nm pump laser diodes as shown in Figure 3.

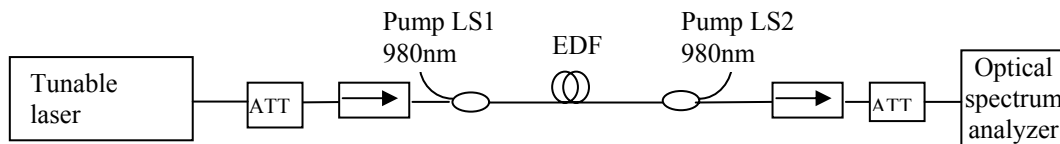


Figure 3 - EDFA measurement setup

The 16m erbium-doped fiber is used as the gain medium, in which the dopant ions absorb the pump photon energy to reach a higher energy state and then translate the stored energy into the incident signal through stimulated emission. The EDF is bi-directionally pumped at 980 nm by two laser diodes LS1 and LS2 in order to obtain the maximum optical power transferred to the signals.

LS1 is a FITEL FOL0906PRO-R17-980 laser diode, and LS2 is PM09GL laser diode of COMSET. The two pump sources are coupled into the gain media through two 980/1550 WDM couplers. The isolators are used to prevent reflection from the output which may cause oscillation in the amplifying medium.

The MG9836A tunable laser is combined with a variable attenuator (ATT) to generate input lightwaves tunable over the whole C-band from 1530 nm to 1565 nm. The output power can be varied from -35 dBm to 8 dBm which has been extended from the original power range of -20 dBm to 8 dBm available from MG9836A. The output of the EDFA is monitored by an AQ6317B optical spectrum analyzer (OSA). Note also that the high output power is attenuated before inserted into the OSA to prevent damage.

3.1.1 ASE spectrum

When the doped ions in the EDF are pumped into excited state they will randomly return to the lower energy level and emit photons even without the input signal, this is the well-known Asynchronous Spontaneous Emission (ASE) phenomenon.

The ASE spectrum can be measured by monitoring the output spectrum of the EDFA while the input signal is turned off.

Figure 4 shows the noise spectrum of the EDFA when a total pump power of 274 mW at 980 nm is injected into the doped fiber. The ASE spectrum peaks at 1530.09 nm and remains flat with a ripple no higher than 0.5 dB over the spectral range from 1537 nm to 1558 nm. Since the spectral distribution density is irregular, the 3-dB bandwidth of the amplifier is not well defined and hence the common definition of 3-dB bandwidth $\Delta\nu$ should not be used. Instead, the bandwidth is determined by evaluating the total noise power over a spectral range and by drawing a box under the ASE curve such that its area is equal to the total noise power and its width has a maximum area overlapping the ASE spectrum. A 36.2 nm 3-dB bandwidth is estimated for our designed optical amplifier.

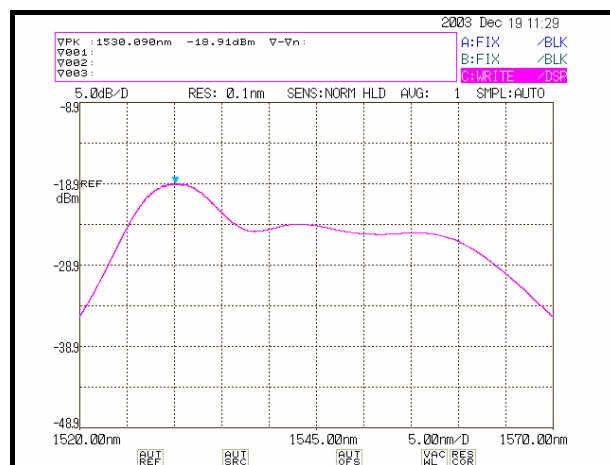


Figure 4 - ASE spectrum

3.1.2 EDFA output power versus input power and power saturation.

Both the EDFA output power and gain are plotted in Figure 5 as a function of the input power with the wavelength as a parameter. The optical output power, hence the gain, is almost indifferent over the spectral range of 1540 nm – 1560 nm. However the gain is increased and decreased by about 4 dB for wavelengths of 1530 nm and 1565 nm respectively. This is consistent with the ASE spectrum shown in Figure 4.

Furthermore, the gain characteristic shown in Figure 5 indicates that for small signal operation the output power (in dB) increases linearly with the increase of input power. For our amplifier, this range is from -35 dBm to -20 dBm. However the onset saturation region varies from -20 dBm to -10 dBm for wavelength range from 1530 nm to 1565 nm. In our mode-locked laser the optical signals are forced to operate in the saturated region.

The gain of the EDFA can be estimated as [12]

$$G = e^{gl} \quad (6)$$

where l is the length of the doped fiber, and g is the gain coefficient given by

$$g = \frac{g_0}{1 + P/P_s} \quad (7)$$

with g_0 is the peak gain value, P is the optical signal average power and P_s is the saturated power level. The gain can be calculated in dB:

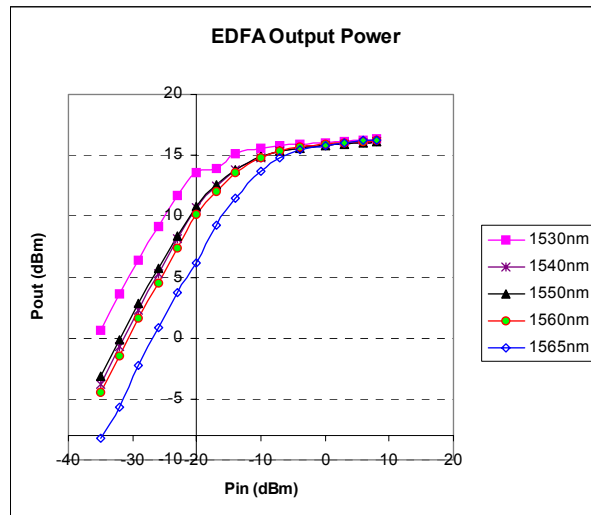
$$G (dB) = 4.343gl \quad (8)$$

Substitute (7) into (8), and note that $P/P_s \gg 1$ in the saturation region we have:

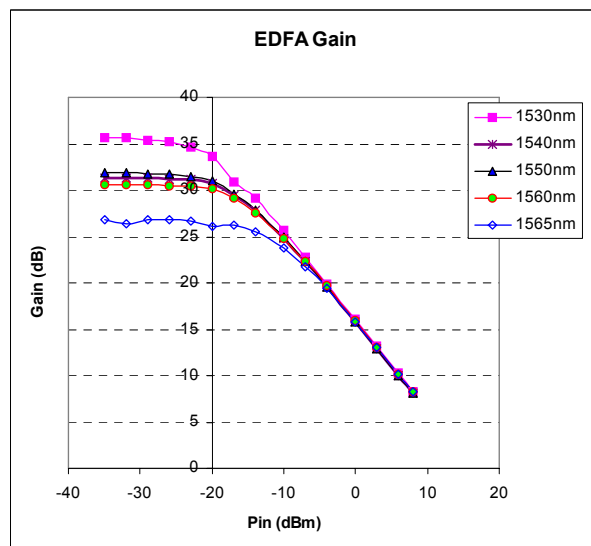
$$G(dB) \approx 4.343l \frac{P_s}{P} \quad (9)$$

The gain decreases proportional to the signal power as it can be seen in Figure 5b.

The highest gain is obtained at 1530 nm while the smallest is at 1565 nm. This agrees with the ASE spectrum shown in Figure 4, where the spectrum peaks at 1530 nm and nearly flats over the range from 1540 nm to 1560 nm, and then drop out when the wavelength increases.



(a)



(b)

Figure 5 - EDFA characteristic. (a) Output power vs input signal power, (b) Amplifier gain vs input power for a doped fiber length of 16 meters.

3.1.3 Gain versus wavelength

Figure 6 shows the gain versus wavelength for the input power P_{in} of -20dBm . It shows that the gain of the EDFA has a small fluctuation or ripple of no higher than 0.8 dB over the entire spectral range of 1540 nm to 1560 nm. The peak of the gain occurs at 1530 nm which is consistent with that observed in the ASE spectrum shown in Figure 4. As previously indicated the ASE spectrum can be alternatively used for a simple estimation of the EDFA bandwidth.

The dependence of the small signal gain G on the wavelength can also be observed in Figure 5 in which the gain at 1530 nm wavelength is maximum. While the gain is almost invariant over the spectral range 1540 nm to 1560 nm, the smallest gain is achieved at 1520 nm. However in the saturated region the optical gain is almost identical for all these spectral regions.

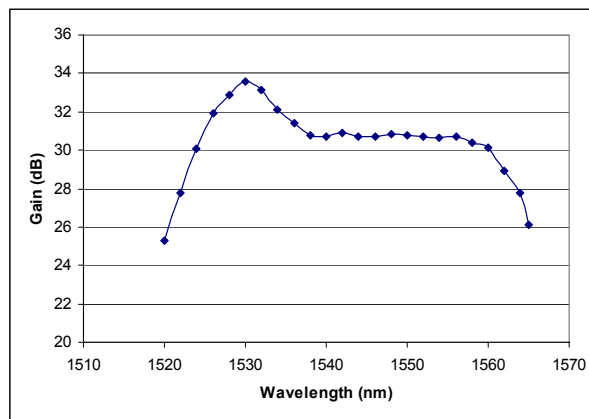


Figure 6 - Gain versus wavelength, $P_{in} = -20dBm$, $P_{pump} = 200mW$

3.1.4 Gain versus pump power

The effect of pump power on the gain is examined by keeping the input signal unchanged and varying the pump power. The gain of the EDFA is determined by monitoring the output power. Figure 7 plots the gain versus the pump power for different input power levels.

Under a small pump power, the gain increases exponentially as indicated by the high gain slope of about 1.5 dB/mW at a power of 13 mW. However the gain slope decreases as the pump power increases and then flattens when the EDFA is pumped into saturation. This is the well-known saturation phenomenon [13, 14]. The pump saturation occurs when all the ions in the EDF are pumped to the excited state. The addition pump power does not contribute any more excited ions, hence there is no increase of the gain factor.

Threshold pump power

Threshold pump power is the required power pumped into the EDFA so that the signal sees the EDFA as transparent, the output power is the same as the input power. Below the threshold power, the signal is attenuated rather than amplified

when traveling through the EDFA due to absorption. The threshold pump power is measured by varying the pump power until the EDFA gain equal to one (i.e. 0dB gain). It can be seen from Table 2 and Figure 7 that the threshold pump power is about 13 mW and unchanged for different input signal power. Thus when pumped with a power of 13 mW the EDFA becomes transparent to the signal regardless of the signal level.

Pump Power (mW)	Gain at different signal powers (dB)		
	Ps = 8dBm	Ps = 0dBm	Ps = -20dBm
10	-2.9	-3.2	-4.6
12	-1.3	-1.6	-2.5
13	-0.5	-0.2	0.1
14	0.1	1.3	1.7
16	1.5	3.2	4.4
18	2.1	5.4	7.5
20	2.7	7.1	10
30	4.3	9.4	16.2
40	5.1	11.6	21.6
50	5.8	12.9	22.4
60	6.4	14.1	22.7
80	7.8	14.7	23.2
120	8.7	15.5	23.79
140	9.3	15.9	24.1
180	9.9	16.4	24.5
200	10.1	16.4	24.8
240	10.2	16.5	25
274	10.3	16.5	25.1

Table 2 - Gain vs pump power for different input levels

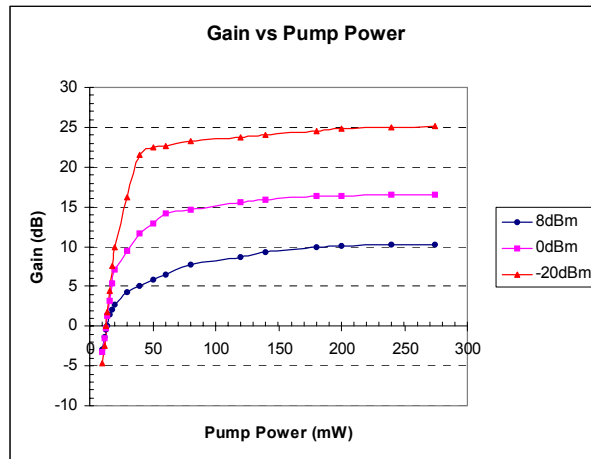


Figure 7 -Gain vs pump power for different input levels

4 Active harmonic mode-locked fiber laser

4.1 Experiment setup

Figure 8 shows the schematic diagram of the active mode-locked fiber laser (MLFL). The fiber ring configuration incorporates an isolator to ensure unidirectional lasing. The gain media is obtained by using a 16 m erbium-doped fiber operating under bi-directional pump condition. The pump sources are two 980 nm laser diodes coupled to the ring through two 980/1550 WDM couplers. A FOL0906PRO-R17-980 laser diode from FITELE is used for the forward pump source and a COMSET PM09GL 980 nm laser diode for the backward pump source. A 18 m long dispersion shifted fiber (DSF) is used for shortening the locked pulse width. A 2 nm bandpass multi-layer thin-film optical filter is used to select the operation wavelength of the laser and moderately accommodate the bandwidth of the output pulses. A polarization controller is also employed to maximize the coupling of lightwaves from fiber to the diffused waveguides of the Mach-Zehnder intensity modulator (MZIM). Output pulse trains are extracted via a 90/10 coupler. Mode locking is obtained by inserting into the ring a 20 GHz 3-dB Mach-Zehnder intensity modulator that periodically modulates the loss of the lightwaves traveling around the ring. The modulator is biased at the quadrature point with a voltage of -1.5V and then driven by superimposing a sinusoidal signal derived from Anritsu 68347C signal generator.

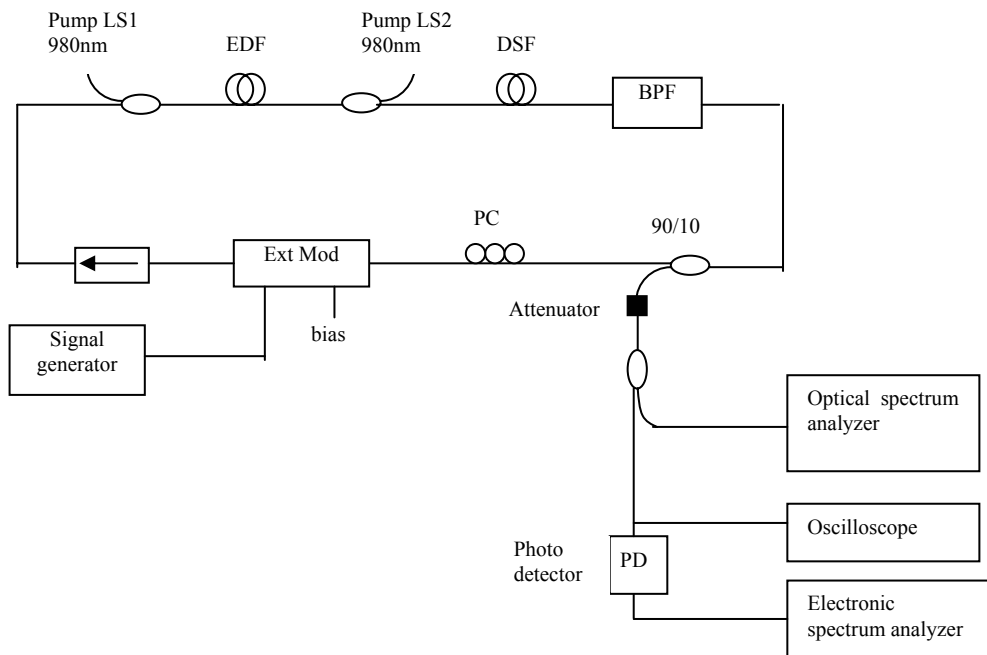


Figure 8 – Active harmonic mode-locked fiber laser experiment setup

The output signal is then monitored using an Agilent 86100B wideband oscilloscope with optical input sampling module, an Ando 6317B optical spectrum analyzer with a resolution of 0.01 nm and an Agilent E4407B electronic spectrum analyzer. Figure 9 shows the picture of the whole system setup for experiment.

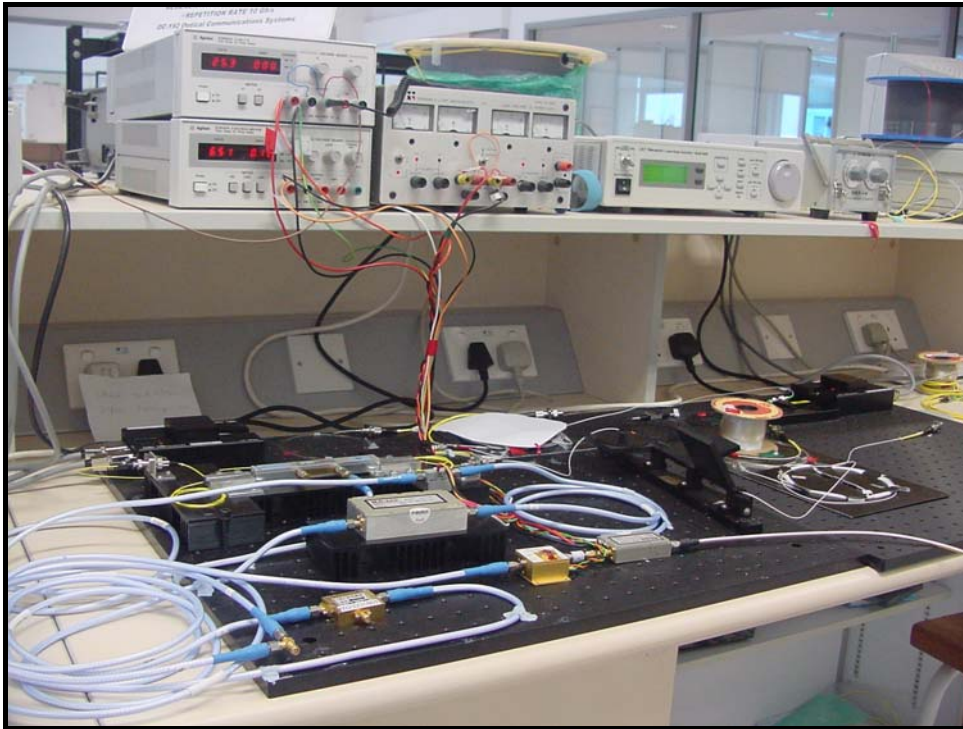


Figure 9 – Active harmonic mode-locked fiber laser

4.2 Tunable wavelength harmonic mode-locked pulses

The total optical cavity length is 55.4 m which corresponding to a fundamental frequency f_R of 3.673 MHz (the measurement of f_R is presented in Section 4.3). When the modulation frequency is set at 2.695038 GHz or equivalently equal to 733 times of f_R , mode locking laser pulse is obtained at the output as shown in Figure 10a. The interval between adjacent pulses is 371 ps, corresponding to a repetition rate of 2.695 GHz. The locked pulses are formed with clear pedestal, with slightly fluctuated amplitude. The output pulse amplitude is measured and a peak power is recorded at 9.9 mW.

The pulse width is also measured and a value of 37 ps full width at half maximum (FWHM) is obtained. However, as this value is taken from the trace of pulse on the oscilloscope the rise time of the oscilloscope is included in the measured value. Since the rise time of the oscilloscope is 20 ps, which is comparable to the measured value, it can not be ignored. Besides that the rise time of the photodiode also contributes to the total measured value. Therefore the actual pulse width is much smaller than the measured value.

Figure 10b shows the optical spectrum of the output pulses. The FWHM bandwidth is 0.137 nm with central wavelength at 1552.926 nm. The time bandwidth product (TBP) was determined as:

$$TBP = T_{FWHM} \times BW \quad (10)$$

$$TBP = 37ps \times 17.125THz = 0.634$$

The large value obtained here again confirms that the measured value of pulse width is mainly contributed by the rise times of oscilloscope and photodiode. The accurate pulse width should be obtained from using an optical auto-correlator.

Alternatively one can take advantage of the characteristic of the AM mode-locked fiber laser to approximate the pulse width. The pulses generated from AM mode-locked fiber lasers are nearly transform limited [15-18]. This means that the TBP takes the value of 0.44, assuming Gaussian shape pulse. Therefore the pulse width can be estimated from:

$$T_{FWHM} = TBP/BW \quad (11)$$

$$T_{FWHM} = 0.44/17.125THz = 26 ps$$

It can be seen from Figure 10b that the pulse train spectrum has sidelobes with a separation of 0.022nm, which corresponds to a longitudinal mode separation of 2.695 GHz. This spectrum profile is typical for the mode-locked laser and usually referred as the mode-locked structure spectrum [11, 19, 20].

The above spectrum profile can be explained by taking the Fourier transform of the periodic Gaussian pulse train:

$$p(t) = e^{-t^2/2T_0^2} * \text{III}\left(\frac{t}{T}\right) \quad (12)$$

where T_0 is the width of the Gaussian pulse, T is the pulse repetition period and $\text{III}(t/T)$ is the comb function given by

$$\text{III}\left(\frac{t}{T}\right) = \sum_{n=-\infty}^{\infty} \delta(t - nT) \quad (13)$$

$$P(\omega) = F(p(t)) = T_0 \sqrt{2\pi} e^{-T_0^2 \omega^2 / 2} \sum_{n=-\infty}^{\infty} \delta(\omega - n\Omega) \quad (14)$$

where $\Omega = 2\pi/T$

$P(\omega)$ has structure of a train of Dirac function pulses separated by the repetition frequency with a Gaussian envelope.

The laser wavelength is tunable over the whole C-band by tuning the central wavelength of the thin film bandpass filter inserted in the loop.

The repetition rate of the laser pulses can be increased by increasing the modulation frequency. Figure 11 shows the output pulses with the repetition rate of 4 GHz and its optical spectrum.

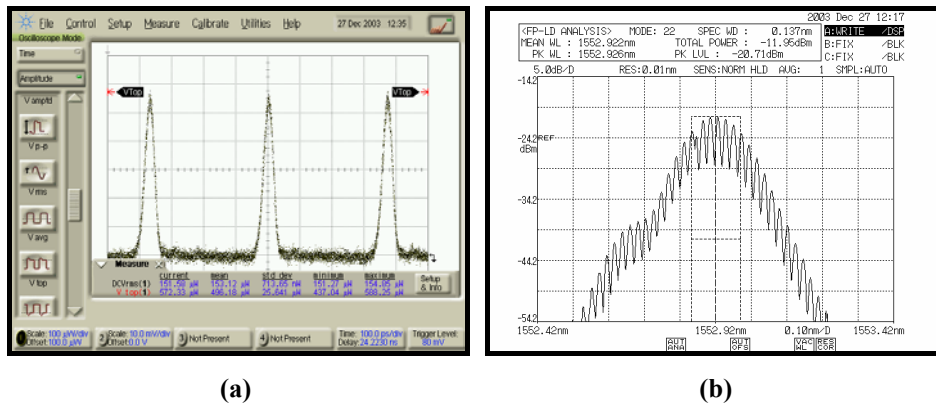


Figure 10 - Harmonic mode-locked pulse train with repetition rate of 2.657GHz (a) and its optical spectrum (b)

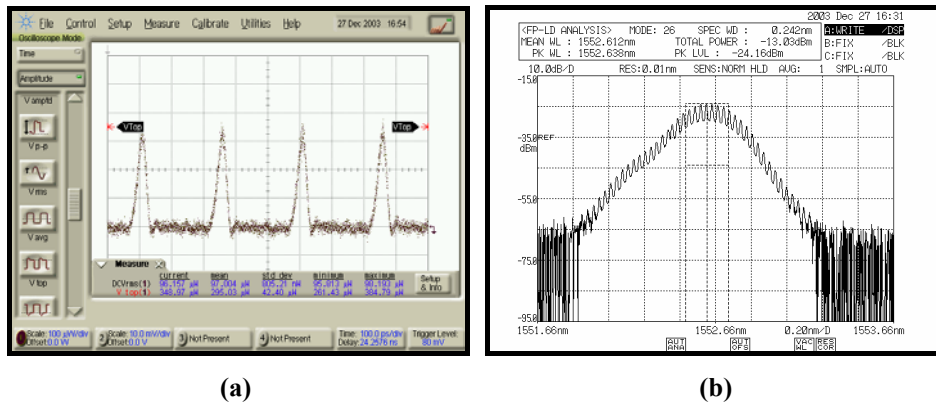


Figure 11 - Harmonic mode-locked pulse train with repetition rate of 4.000GHz; (a) temporal profile, (b) optical spectrum .

4.3 Measurement of fundamental frequency

In active harmonic mode-locked fiber laser (HMLFL) the pulses are locked into one of the harmonic of the fundamental frequency f_R by tuning the modulation

frequency f_m so that $f_m = kf_R$. In practice, the laser is mode-locked if f_m is within the locking range around the harmonic frequency, that is $f_m = kf_R \pm \Delta f$. If f_m falls outside the locking range the laser becomes unlocked, that is no pulse trains are observed. If f_m is adjusted until reaching the next harmonic frequency $(k+1)f_R$, the HMLFL is locked again into the next longitudinal resonant mode of the ring. By measuring those locked modulation frequencies, one can determine the fundamental frequency of the ring. Table 3 shows the results of measuring eleven consecutive locking frequencies and their lower and upper locking limits. The fundamental frequency is determined by:

$$(4018635400 - 3981902400)/10 \text{ Hz} \leq f_R \leq (4018636000 - 3981901400)/10 \text{ Hz}$$

$$3673300 \text{ Hz} \leq f_R \leq 3673460 \text{ Hz}$$

or

$$f_R = 3673380 \pm 80 \text{ Hz}$$

Lowest Locking Frequency (Hz)	Highest Locking Frequency (Hz)	Locking Frequency (Hz)	Locking Range (Hz)	Harmonic order
3981901400	3981902400	3981901900	1000	1084
3985569400	3985569800	3985569600	400	1085
3989253300	3989254100	3989253700	800	1086
3992928600	3992929900	3992929250	1300	1087
3996601700	3996602400	3996602050	700	1088
4000285600	4000285800	4000285700	200	1089
4003963700	4003964200	4003963950	500	1090
4007641900	4007642600	4007642250	700	1091
4011319700	4011320500	4011320100	800	1092
4014979600	4014980300	4014979950	700	1093
4018635400	4018636000	4018635700	600	1094

Table 3 - Locking modulation frequencies and locking ranges

4.4 Effect of the modulation frequency

Increasing modulation frequency not only generates higher repetition rate mode-locked pulses but also improves other parameters of the pulses such as bandwidth, pulse width.

The solid curve shown in Figure 12 indicates the relationship between the pulse width of the generated pulse train and modulation frequency. The pulse width does not change so much when the modulation frequency increase above 2 GHz. This is because the pulse width in this region is small comparable to the rise time of the oscilloscope. The actual values should be smaller than the measured values. This is confirmed when examining the equivalent bandwidth of the pulse trains.

Figure 13 shows the pulse train bandwidth versus the modulation frequency. The modulation frequency increases the bandwidth increases. Unlike the behavior of pulse width, the pulse train bandwidth continues to increase even when the modulation frequency is above 2 GHz. This indicates that the actual pulse width should be smaller than its measured value. The pulse width is calculated using equation (11) and plotted as shown by the dash curve in Figure 12.

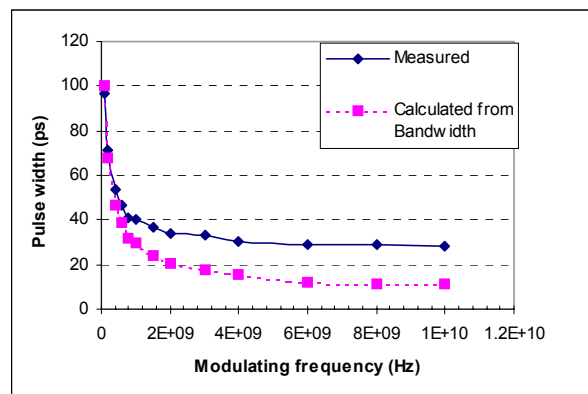


Figure 12 - Pulse width of the HMLFL for various modulation frequencies

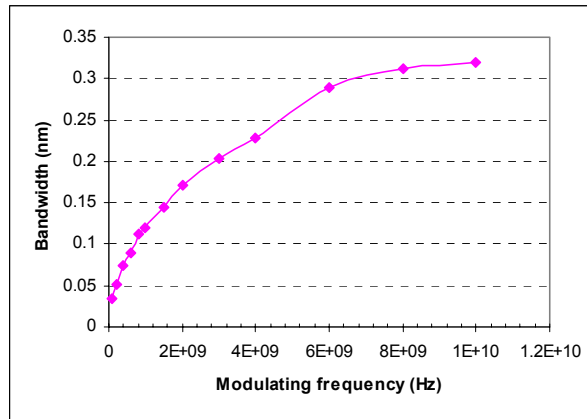


Figure 13 - Bandwidth of the HMLFL for various modulation frequencies

4.5 Effect of the modulation depth/index

The same setup as shown in Figure 8 has been used to study the effect of modulation depth on the performance of the mode-locked pulse trains. The settings of the cavity are as following: (i) the total pump power is 274 mW (ii) the modulator is biased at the quadrature point. The modulation depth is varied by changing the signal amplitude (from the signal synthesizer) applied to the MZIM. The pulse width and bandwidth of the output pulse trains are measured for different values of modulation depth.

Figure 14 shows the relationship between pulse width and modulation amplitude/power. As the modulation power increases the pulse width slightly decreases. Therefore the pulse can be shortened by increasing the modulation power (or the modulation depth). However the pulse shortening effect of modulation depth is not as strong as that of modulation frequency. In addition, the modulation depth is limited to a maximum value of 1.

The relationship between pulse width and the modulation depth is verified by examining the effect of modulation power on the bandwidth. When the modulation power increases the bandwidth decreases as shown in Figure 15. This is consistent with the decrease of pulse width shown in Figure 14.

It is found that there is a threshold power of the modulation for locking. When the modulation power is reduced to -4 dBm corresponding to a modulation depth of 0.08, mode locking does not occur and pulse train cannot be obtained.

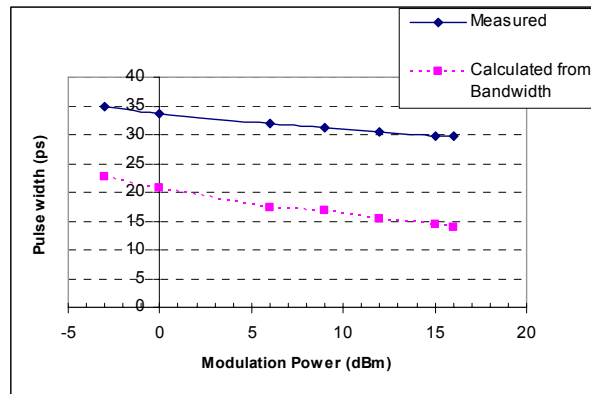


Figure 14 - Pulse width of the HMLFL for various modulation powers

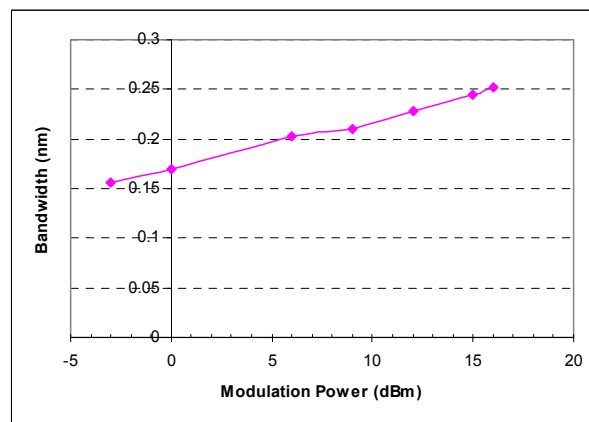


Figure 15 - Bandwidth of the HMLFL for various modulation powers

4.6 Effect of fiber ring length

The same set up as in Figure 8 has been used to study the effect of the fiber ring length on the mode-locked pulse trains. The DSF fiber has been extended from 18 m to 118 m. A total pump power of 274 mW is used. The pulse width and bandwidth have been measured and compared with those described in Section 4.2. Figures 16 and 17 show the mode-locked pulse temporal train and its optical spectrum for the 18m DSF ring laser and the 118m DSF ring laser respectively.

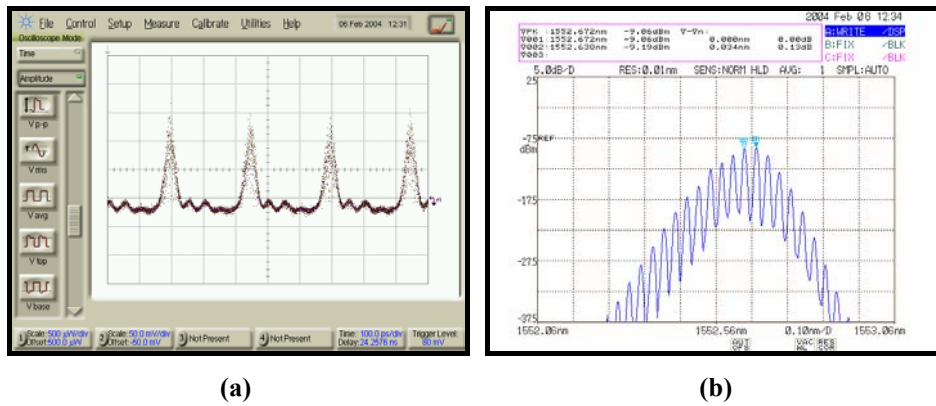


Figure 16 - Locked pulses (a) and its optical spectrum (b) for the 18m DSF ring laser

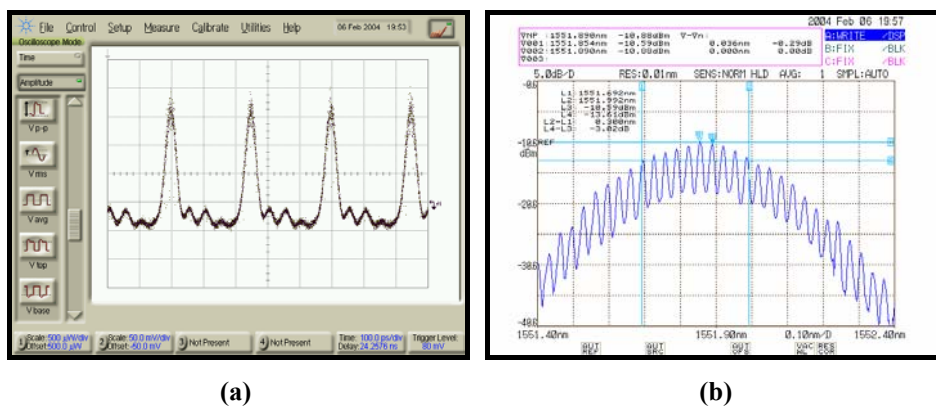


Figure 17 - Locked pulses (a) and its optical spectrum (b) for the 118m DSF ring laser

The pulse trains are very much similar for both cases. Their pulse widths (FWHM) are nearly equal, 33 ps and 29 ps. However the pulse optical spectra are quite different, The longer ring laser has a bandwidth of 3 nm, larger than that of the shorter one, 0.184 nm. The broadening of the bandwidth of the pulse train of the 110 m ring length indicates that the pulse width is shorter than what it is observed by the sampling oscilloscope. The discrepancy here is again due to the affect of the photodiode and oscilloscope's rise time on the observed pulse.

The shortening of the pulse in the longer length ring can be due to the self phase modulation (SPM) effects or the nonlinear induced phase in the fiber. The high intensity pulse traveling in the fiber is suffered the nonlinear effect which increases the peak of the pulse, shortens the pulse width and hence the bandwidth broadening.

To verify that the pulse shortening is due to the nonlinear effect, the two different length rings are studied under lower pump power. It is found that when the pump power is reduced to 50 mW, the pulse width and bandwidth of the laser does not change regardless of the fiber length.

One can estimate the effective nonlinear lengths of the fiber for the pump power of 274 mW and 50 mW. The peak pulse powers are 0.37 W and 0.027 W respectively. The nonlinear lengths can be calculated as [21]:

$$L_{NL}(P_p = 274mW) = \frac{1}{\gamma P_0} = \frac{1}{2 \times 10^{-3} \times 0.37} = 1351(m) \quad (15)$$

$$L_{NL}(P_p = 27mW) = \frac{1}{\gamma P_0} = \frac{1}{2 \times 10^{-3} \times 0.027} = 18518(m) \quad (16)$$

It can be seen that the effective nonlinear length of the 118 m long fiber ring is comparable to that of the physical ring length when pumped at high power. Therefore the nonlinear effect plays a significant role in this case. When the laser is pumped at lower power, the effective nonlinear length is much longer than the laser ring length, hence the SPM effect is minute and can not be observed. However, one can predict the existence of the SPM effect if the fiber length is increased to be comparable with the nonlinear length.

It is also noticed that the super-mode noise was reduced in the case of longer fiber ring. The pulses are more temporally stable and less fluctuating. To verify this, the RF spectrum of the lasers are recorded and compared. It can be seen from Figure 18 that the longer length laser has a lower noise floor than the shorter one.

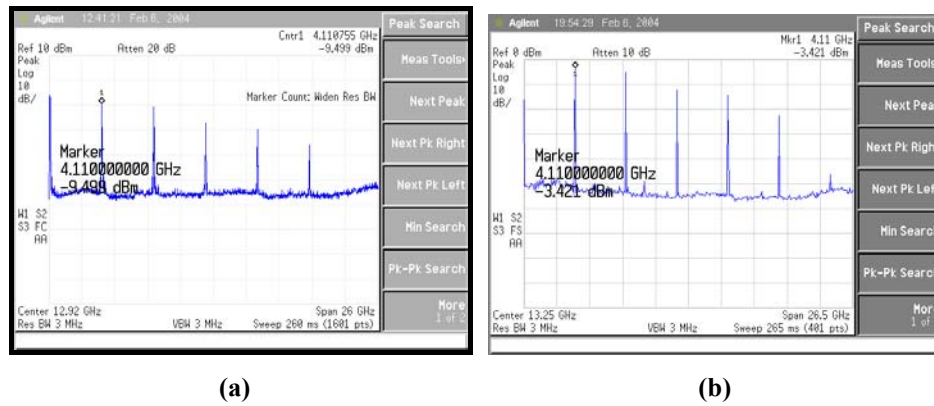


Figure 18 - RF spectrum of HML laser with 18m DSF (a), and 118m DSF (b)

4.7 Effect of pump power

The laser is configured as in Figure 8 except that the fiber length is 118m. Different power levels are pumped into the EDFA to study the laser performance. Figure 19 shows the variation of the laser pulse widths under various pump powers. The pulse widths seem to be slightly affected by the change of pump power. However, the affect of the pump power is actually stronger since the pulse widths measured here are not the true pulse widths. They are larger than their true values due to the rise time of the equipment as discussed above. The affect of pump power on the pulse width can be drawn from the relationship between pump power and output pulse bandwidth.

The dependence of the output pulse bandwidth is illustrated in Figure 20. As the pump power increases the bandwidth increases. Since the bandwidth is inverse proportional to the pulse width, one can infer that the pulse width decreases when the pump power increases. The cause of the decrease in pulse width is attributed to the nonlinear effect. The higher the peak power the stronger the nonlinear effect, hence the shorter pulse width. It is also noticed that the pulse shortening effect of the pump power is only observed when the fiber length is long comparable to the effective nonlinear length as discussed in Section 4.6

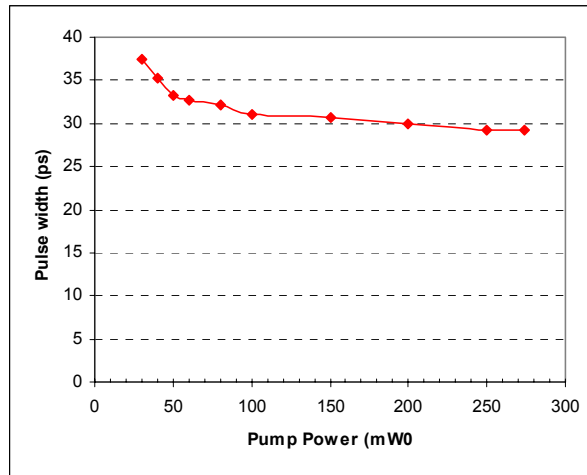


Figure 19 - Pulse width of the HMLFL for various pump powers

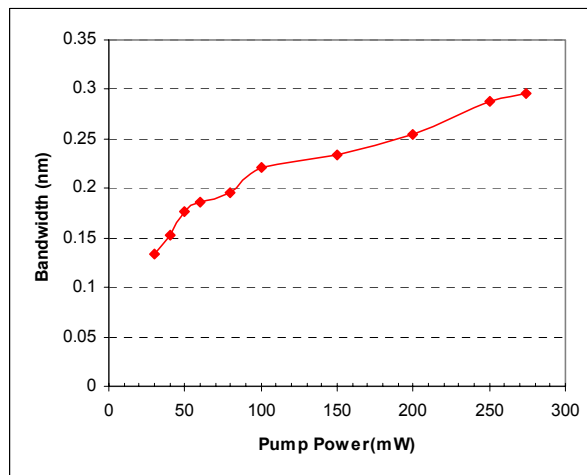


Figure 20 - Bandwidth of the HMLFL for various pump powers

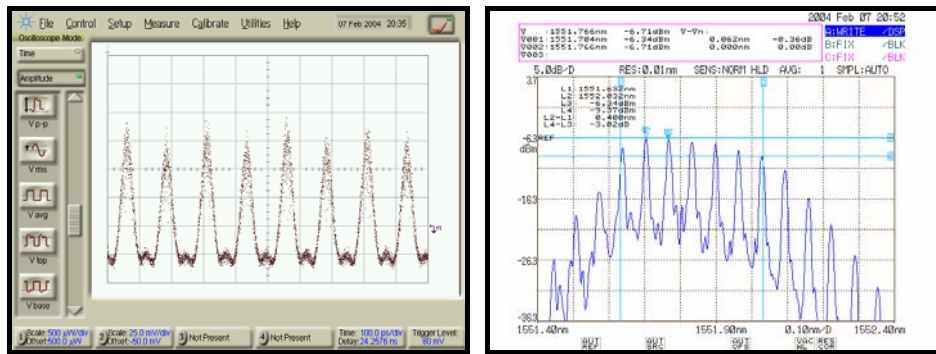
4.8 Multiplication of repetition rate by detuning

The repetition rate of the active mode-locked fiber laser is determined by the modulation frequency applied to the MZI modulator. The highest modulation frequency can be used for mode locking is certainly limited by the MZI modulator. The current fastest modulator can operate with a 3 dB bandwidth up to 40 GHz. Therefore the repetition rate of active mode-locked laser is normally limited at 40 GHz. To obtain higher repetition rate the rational harmonic mode-locking (RHML) technique should be used. In RHML laser, the modulation frequency is not an integer number harmonic of the fundamental frequency f_R but detuned by an amount of f_R/N

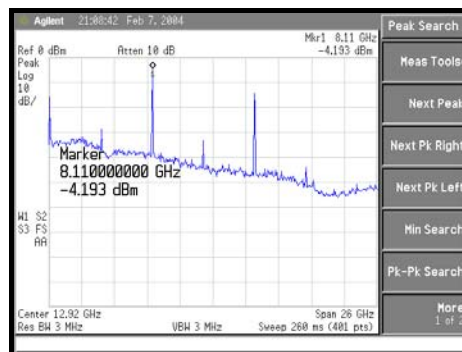
$$f_m = mf_R + f_R/N \tag{17}$$

where m and N are integer numbers and N is defined as the multiplying factor. The output pulse repetition rate is now no longer f_m but Nf_m . In another word, it has been multiplied by N .

Figure 21a shows the output pulse train of the mode-locked laser when the modulation frequency is set to 4.047327 GHz, that is equal to $f_R + f_R/2$. The pulse period is 123 ps which corresponds to a repetition rate of 8.094 GHz. It means doubling the repetition rate. Mode-locking at 8.094 GHz can be confirmed by observing the optical spectrum of the pulse train shown in Figure 21b. Separation between two harmonic peaks is 0.062 nm corresponding to a repetition rate of 8.094 GHz. The RF spectrum of the pulse observed at the output of the fast photodiode is also illustrated on Figure 21c. The peak at 8.094 GHz again confirms the laser is locked at the repetition rate of 8.094 GHz.



(a) (b)



(c)

Figure 21 - Doubling repetition rate by detuning; (a) locked pulses, (b) optical spectrum, and (c) Rf spectrum

The three times and four times repetition rate multiplying effects are also observed in our fiber ring laser. Figures 22 and 23 show the output pulses when the modulation frequencies are 4.047116 GHz and 4.047010 GHz respectively. However, the pulses are less stable than that of repetition rate doubling. They are so fluctuating due to pulse dropping effects. The pulse peak powers also vary from pulse to pulse. This is one of the disadvantages of the RHML technique [22, 23].

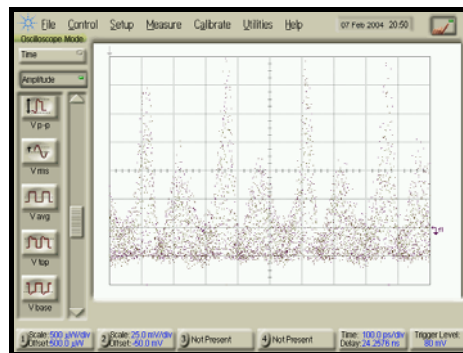


Figure 22 - Tripling repetition rate by detuning the modulation frequency by $f_R/3$

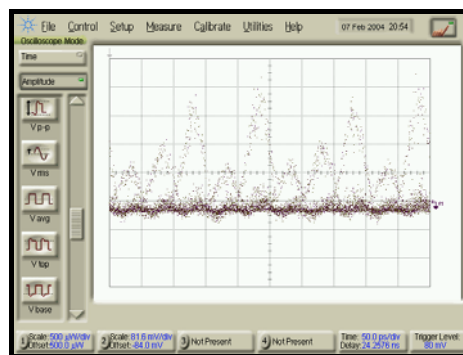


Figure 23 - Quadrupling repetition rate by detuning the modulation frequency by $f_R/4$

4.9 Regenerative harmonic mode-locked fiber laser

One of the disadvantages of harmonic mode-locked fiber laser is its sensitivity to the change of the environment, especially due to temperature fluctuation. The length of the fiber varies with the temperature and causes a change in the fundamental locking frequency. Therefore the modulation frequency is no longer

a harmonic of the fundamental frequency and the locking condition is not satisfied. The laser is thus not stable.

To stabilize the laser the temperature should be kept unchanged or the fiber length should be compensated for temperature variation. The fiber can be wound on a PZT to control the length [11, 24]. The output of the laser is monitored and feed back to the PZT to adjust the fiber length.

Alternatively the harmonic mode-locked laser can be stabilized using the regenerative harmonic mode-lock technique. In this technique, the modulation frequency is not independent to the fundamental frequency but controlled and generated by using a feedback mechanism. Therefore the modulation frequency can be kept at a value equal to the harmonic of the fundamental frequency regardless of any change of the fiber length. Figure 24 shows the schematic diagram of the experimental set up of the regenerative harmonic mode-locked fiber laser.

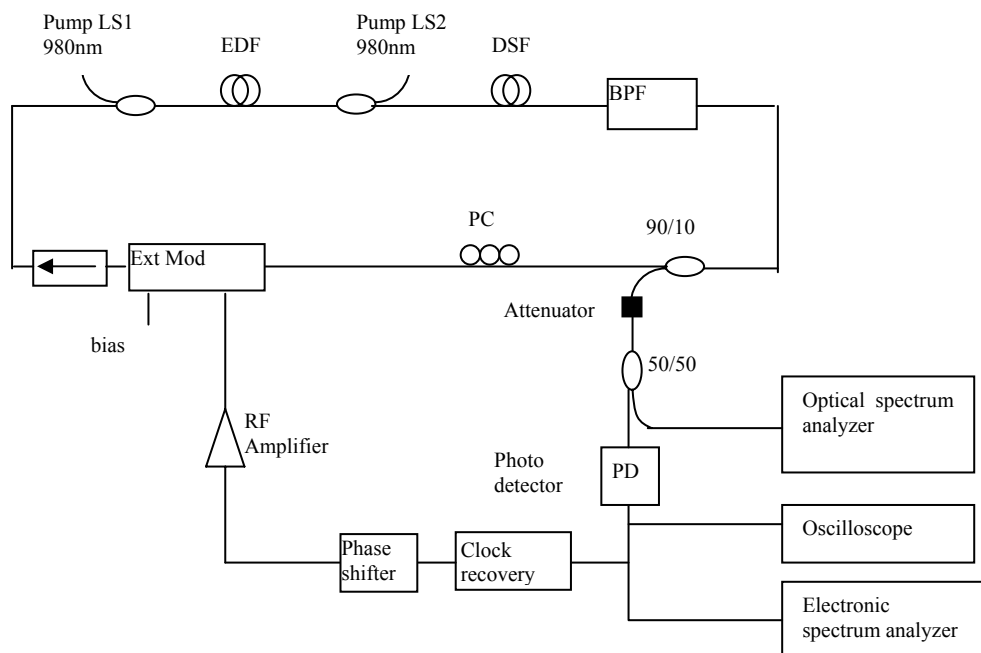


Figure 24 - Regenerative harmonic mode-locked fiber laser setup

The setup is similar to the harmonic mode-locked fiber laser shown in Figure 8 except that the modulation signal is extracted from the output of the laser itself. The output pulses are detected using a New Focus 0178B photo detector (PD) and monitored using an Agilent E4407B electronic spectrum analyzer and a Tektronik CSA8000 Communication Signal Analyzer/Oscilloscope. The electrical output

pulses from the photo detector (PD) are fed into the clock recovery to extract the repetition frequency of the pulses. The recovered signal at the output is used to control the modulator after amplified and phase shifted. The phase offset between the pulses and the modulation signal is adjusted by the phase shifter so that the pulses always experience the optimum loss when they pass through the modulator.

Figure 25 shows the output pulses of the laser without the regenerative feedback loop. The laser is locked and generates pulse train at 10 GHz repetition rate as seen in the figure when a 10 GHz sin wave signal is applied into the modulator. However, the pulses have been stable for just about half an hour and then blur out due to the variation of the environment. Clear mode-locked pulses are only obtained when the modulation frequency is properly tuned again.

When the regenerative feedback loop is closed and the phase shifter is properly adjusted, a stable and well defined shape pulse train is obtained at the output without the need of external modulation signal as shown in Figure 26. The mode-locked pulse train has been observed for several hours without the need of retuning. The recovered modulation signal has been automatically adjusted through the regenerative loop to adapt to the change of the cavity length due to the variation of the environment.

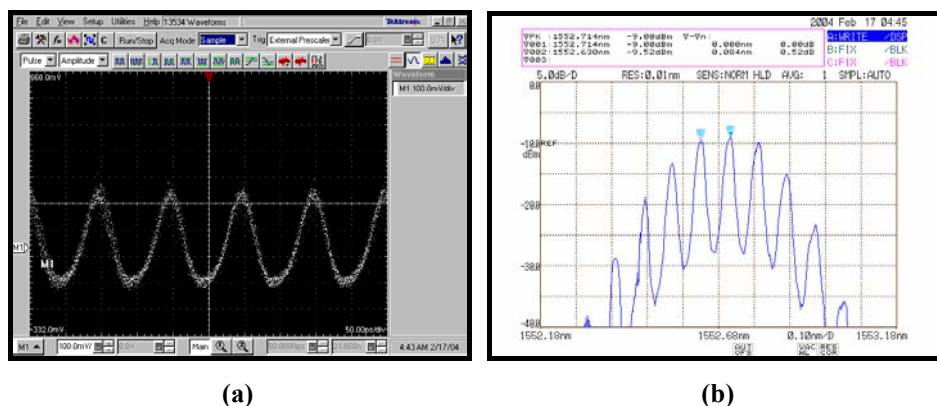


Figure 25 - Harmonic mode-locked fiber laser with 10GHz repetition rate;(a) temporal pulse train, (b) optical spectrum

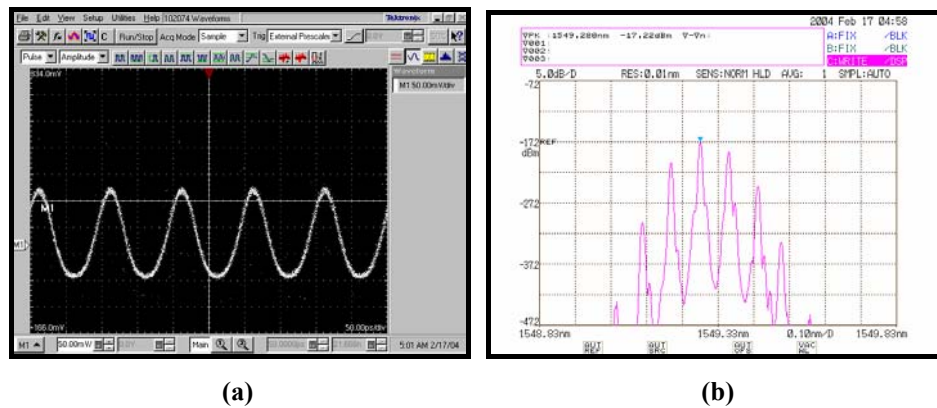


Figure 26 - Regenerative harmonic mode-locked fiber laser with 10GHz repetition rate;(a) temporal pulse train, (b) optical spectrum

4.10 “Giant” pulse locking

While studying the characteristics of mode-locked fiber ring laser, we observed a new phenomenon, which is called “giant” pulse locking. “Giant” pulse locking is referred to the phenomenon in which the mode-locked pulses have much higher peak power than that of the normal mode-locked pulses. The laser setup is the same as shown in Figure 8. When the modulation frequency is 2.695038 GHz mode locking laser pulses are obtained at the output as shown in Figure 27. The characteristics of the pulses have been discussed in section 4.2.

When the modulation frequency is detuned by 10 kHz to 2.695048 GHz, locking laser pulses are obtained but the pulses have a pedestal as observed in Figure 28a. The peak pulse amplitude is very high. It was measured as high as 57.5 mW, nearly six times that of normal locking (9.9 mW). This peak power corresponds to an estimate 575 mW peak power of the pulses traveling inside the ring laser.

The pedestal may be due to pulse dropout, some pulses may have been dropped out in the ring and these pulses are captured on oscilloscope as the bottom lines similar to the pulse trains of return-to-zero (RZ) format as usually observed in optical transmission system.

Figure 28b shows the output optical spectrum of the “giant” pulse locking laser. It is interesting that the spectrum is smooth and no sidelobes of the carrier-modulated pulse train are recorded. This can be explained as follow. In harmonic mode-locked fiber laser which is locked to the N^{th} harmonic of the fundamental

frequency f_F , there are N sets of longitudinal modes called super-modes. Those super-modes compete with each other and hence the laser may be switched to oscillate from one set to another. Frequency separation of those super-modes is equal to f_F . In this experiment, f_F is 3.667 MHz, quite smaller than the resolution of optical spectrum analyzer (0.01 nm). Therefore the sidelobes of those super-modes cannot be distinguished on the spectrum analyzer.

Although the underlying physical mechanism of this phenomenon is still not explained, we believe that the super-mode competition and the relaxation time of the optical amplification in the ring may be the reasons of pulse drop-out phenomenon that we have observed in the time domain. Further investigation to this phenomenon is out of scope of this paper and is left for future research.

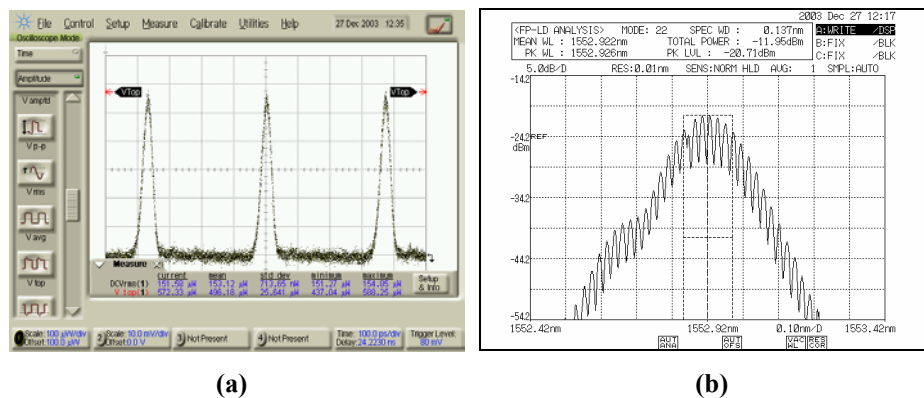


Figure 27 - Mode-locked pulse train with clear pedestal (a) and its optical spectrum (b)

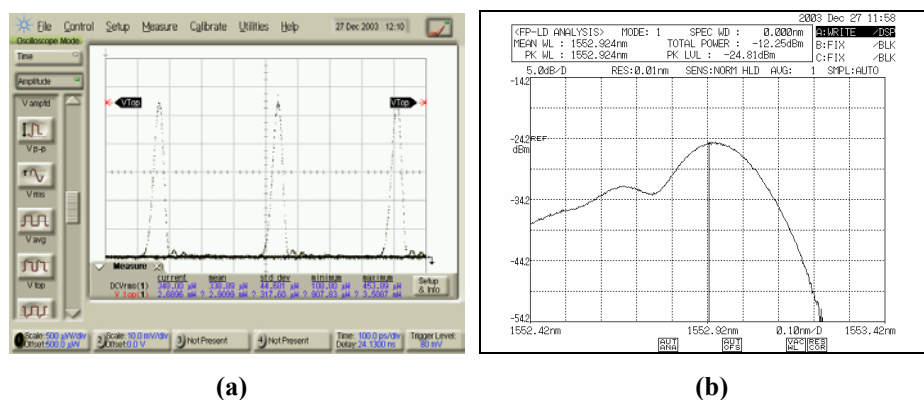


Figure 28 – “Giant” (high peak power) optical pulse train observed at the output of harmonic mode-locked laser when the modulation frequency is detuned by about 10 kHz (a) temporal pulse trains (b) pulse train spectrum.

5 Conclusions

In this paper three types of mode-locked lasers have been successfully demonstrated together with the characterization of active photonic elements. The optical transmission transfer characteristic of the MZI modulator has been measured. It is found that the characteristic of the MZI modulator is close to the specification of the manufacturer except a little degradation in insertion loss and extinction ratio. The DC drift of the maximum transmission point is also confirmed.

The EDFA has also been implemented and tested. Its ASE spectrum has been obtained and the EDFA bandwidth has also been measured. The dependence of the gain on the signal wavelength, signal power and pump power has been explored. It is found that the EDFA gain varies with the wavelength over the C-band, peaks at 1530nm, nearly flats from 1540nm to 1560nm, decreases rapidly at 1525nm and 1565nm. However, the gain does not vary so much with the wavelength when it operates in the saturation region, when the input signal power is greater than -10 dBm for our designed EDFA.

The pulse train of very short pulse width at high repetition rate, up to 10GHz, generated from a HMLFL has been demonstrated. The characteristics of the pulse train such as pulse width and bandwidth have been studied by varying the settings of the cavity. It is found that as the modulation frequency increases the pulse becomes shorter and its corresponding bandwidth increases. The increase of the modulation depth also makes the pulse shorter but its effect on the pulse is not as strong as modulation frequency. High pump power is also found to help shorten the pulse width in the long cavity laser.

Multiplication of the repetition rate in the HMLFL by detuning the modulation frequency has also been investigated. Stable doubling of the repetition rate of mode-locked pulse train has been obtained when the modulation frequency is detuned by a half of the fundamental frequency. The pulse amplitude fluctuates from pulse to pulse. Tripling and quadrupling multiplication rate have also been observed but the output pulses are not as stable as that of the doubling case.

Finally, the mode-locked pulse trains have been stabilized using regenerative feedback mechanism. The output pulse trains of the RHMLFL have been proven to be very stable against the variation of the environment for several hours without the need of retuning the modulation frequency.

We also observe a new phenomenon, the “giant” (high peak power, in order of 500 mW) pulse train is generated from a harmonic mode locked laser when it is detuned from the mode-locked frequency of about 10 kHz. Further investigation of this phenomenon is essential and further studies are recommended for clarification. However we believe that this may be due to the super-mode competition and the relaxation of the optical amplification process in the EDFA incorporated in the laser ring.

Readers can refer to another technical report posted on the same website on numerical modeling of mode-locked lasers to compare with those results reported in this document.

References

- [1] K. Gurs and R. Murrler, "Beats and modulation in optical ruby lasers," presented at Quantum Electronics, 1964.
- [2] H. A. Haus, "Mode-locking of lasers," *Selected Topics in Quantum Electronics, IEEE Journal of*, vol. 6, pp. 1173-1185, 2000.
- [3] C. V. Shank and E. P. Ippen, "Subpicosecond kilowatt pulses from a mode-locked cw dye laser," *Applied Physics Letters*, vol. 24, pp. 373-375, 1974.
- [4] R. L. Fork, B. I. Greene, and C. V. Shank, "Generation of optical pulses shorter than 0.1 psec by colliding pulse mode locking," *Applied Physics Letters*, vol. 38, pp. 671-672, 1981.
- [5] J. G. Fujimoto, A. M. Weiner, and E. P. Ippen, "Generation and measurement of optical pulses as short as 16 fs," *Applied Physics Letters*, vol. 44, pp. 832-834, 1984.
- [6] R. L. Fork, C. H. B. Cruz, P. C. Becker, and C. V. Shank, "Compression of optical pulses to six femtoseconds by using cubic phase compensation," *Optics Letters*, vol. 12, pp. 483, 1987.
- [7] U. Morgner, F. X. Krtner, S. H. Cho, Y. Chen, H. A. Haus, J. G. Fujimoto, E. P. Ippen, V. Scheuer, G. Angelow, and T. Tschudi, "Sub-two-cycle pulses from a Kerr-lens mode-locked Tisapphire laser," *Optics Letters*, vol. 24, 1999.
- [8] G. Zhu, Q. Wang, H. Chen, H. Dong, and N. K. Dutta, "High-quality optical pulse train generation at 80 Gb/s using a modified regenerative-

- type mode-locked fiber laser," *Quantum Electronics, IEEE Journal of*, vol. 40, pp. 721-725, 2004.
- [9] G. Lin, J. Wu, and Y. Chang, "40 GHz rational harmonic mode-locking of erbium-doped fiber laser with optical pulse injection," presented at Optical Fiber Communications Conference, 2003. OFC 2003, 2003.
- [10] Y. D. Gong, P. Shum, M. K. Rao, C. Lu, T. H. Cheng, Q. Wen, and D. Y. Tang, "Novel cavity length feedback and stable operation of actively mode locked fiber ring laser," presented at Microwave and Millimeter Wave Technology, 2002. Proceedings. ICMMT 2002. 2002 3rd International Conference on, 2002.
- [11] M. Nakazawa and E. Yoshida, "A 40-GHz 850-fs regeneratively FM mode-locked polarization-maintaining erbium fiber ring laser," *Photonics Technology Letters, IEEE*, vol. 12, pp. 1613-1615, 2000.
- [12] G. P. Agrawal, *Applications of Nonlinear Fiber Optics*, 2001.
- [13] M. A. Mahdi, S. Selvakennedy, P. Poopalan, and H. Ahmad, "Saturation parameters of erbium doped fibre amplifiers," presented at Semiconductor Electronics, 1998. Proceedings. ICSE '98. 1998 IEEE International Conference on, 1998.
- [14] G. R. Walker, "Gain and noise characterisation of erbium doped fibre amplifiers," *Electronics Letters*, vol. 27, pp. 744-745, 1991.
- [15] D. Kuizenga and A. Siegman, "FM and AM mode locking of the homogeneous laser--Part II: Experimental results in a Nd:YAG laser with internal FM modulation," *Quantum Electronics, IEEE Journal of*, vol. 6, pp. 709-715, 1970.
- [16] D. Kuizenga and A. Siegman, "FM and AM mode locking of the homogeneous laser--Part I: Theory," *Quantum Electronics, IEEE Journal of*, vol. 6, pp. 694-708, 1970.
- [17] M. Nakazawa, "Ultrafast optical pulses and solitons for advanced communications," presented at Lasers and Electro-Optics, 2003. CLEO/Pacific Rim 2003. The 5th Pacific Rim Conference on, 2003.
- [18] M.-Y. Jeon, H. K. Lee, K. H. Kim, E.-H. Lee, S. H. Yun, B. Y. Kim, and Y. W. Koh, "An electronically wavelength-tunable mode-locked fiber laser using an all-fiber acoustooptic tunable filter," *Photonics Technology Letters, IEEE*, vol. 8, pp. 1618-1620, 1996.
- [19] T. Pfeiffer and G. Veith, "40 GHz pulse generation using a widely tunable all-polarisation preserving erbium fibre ring laser," *Electronics Letters*, vol. 29, pp. 1849-1850, 1993.
- [20] H. Takara, S. Kawanishi, M. Saruwatari, and K. Noguchi, "Generation of highly stable 20 GHz transform-limited optical pulses from actively mode-locked Er³⁺-doped fibre lasers with an all-polarisation maintaining ring cavity," *Electronics Letters*, vol. 28, pp. 2095-2096, 1992.
- [21] G. P. Agrawal, *Nonlinear Fiber Optics*, 2001.
- [22] M.-Y. Jeon, H. K. Lee, J. T. Ahn, D. S. Lim, H. Y. Kim, K. H. Kim, and E.-H. Lee, "Amplitude equalization of laser pulses obtained from rational harmonic mode locking of a ring-type fiber laser," presented at Lasers and Electro-Optics, 1998. CLEO 98. Technical Digest. Summaries of papers presented at the Conference on, 1998.
- [23] D. L. A. Seixas and M. C. R. Carvalho, "50 GHz fiber ring laser using rational harmonic mode-locking," presented at Microwave and

- Optoelectronics Conference, 2001. IMOC 2001.Proceedings of the 2001 SBMO/IEEE MTT-S International, 2001.
- [24] M. Nakazawa, E. Yoshida, and K. Tamura, "Ideal phase-locked-loop (PLL) operation of a 10 GHz erbium-doped fibre laser using regenerative modelocking as an optical voltage controlled oscillator," *Electronics Letters*, vol. 33, pp. 1318-1320, 1997.